Functional Characterization of Melanocortin-3 Receptor In Rainbow Trout (*Oncorhynchus Mykiss*)

Hui-Xia Yu
Northwest A&F University: Northwest Agriculture and Forestry University
Yang Li
Northwest A&F University: Northwest Agriculture and Forestry University
Wei-Jia Song
Northwest A&F University: Northwest Agriculture and Forestry University
Hui Wang
Northwest A&F University: Northwest Agriculture and Forestry University
Hao-Lin Mo
Northwest A&F University: Northwest Agriculture and Forestry University
Qiao Liu
Air Force Medical University Tangdu Hospital
Xin-Miao Zhang
Northwest A&F University: Northwest Agriculture and Forestry University
Ze-Bin Jiang
Northwest A&F University: Northwest Agriculture and Forestry University
Li-Xin Wang (fisherwanglx@nwafu.edu.cn)
Northwest A&F University: Northwest Agriculture and Forestry University

Research Article

Keywords: Rainbow trout, Melanocortin-3 receptor, Molecular cloning, Tissue expression, Signaling

Posted Date: May 13th, 2021

DOI: https://doi.org/10.21203/rs.3.rs-507819/v1

Version of Record: A version of this preprint was published at Fish Physiology and Biochemistry on January 31st, 2022. See the published version at https://doi.org/10.1007/s10695-021-01033-5.

Abstract

The melanocortin-3 receptor (MC3R) is an important regulator of energy homeostasis and inflammation in mammals. However, its function in teleost fish needs to be further explored. In this study, we characterized rainbow trout MC3R (rtMC3R), which encoded a putative protein of 331 amino acids. Phylogenetic and chromosomal synteny analyses showed that rtMC3R was closely related to bony fishes. Quantitative PCR (qPCR) revealed that the transcripts of rtMC3R were highly expressed in the brain and muscle. The cellular function of rtMC3R was further verified by the signal-pathway-specific luciferase reporter assays. Four agonists such as α-MSH, β-MSH, ACTH (1–24) and NDP-MSH can active rtMC3R, increasing the production of intracellular cAMP and up-regulating MAPK/ERK signals. Moreover, we found that rtMC3R stimulated with α-MSH and NDP-MSH can significantly inhibit the NF-κB signaling pathway. This research will be helpful for further studies on the function of *MC3R* in rainbow trout, especially the role of energy metabolism and immune regulation.

Introduction

Melanocortin receptors (MCRs) belong to the class A rhodopsin family of G protein-coupled receptors (GPCRs). Up to date, five members of melanocortin receptors have been identified in mammals, which were named MC1R-MC5R in the order of discovery (Gantz and Fong 2003). Although they all had 7 conserved transmembrane domains (TMDs) in structure and can be activated by corresponding melanocortins, such as α-MSH, β-MSH, ACTH, etc., the tissue expression and cellular function of each receptor were different (Novoselova et al. 2018). Among them, MC3R and MC4R were two subtypes mainly expressed in the central nervous system, involving the regulation of energy homeostasis. In humans, it had been found that the mutations of *MC3R* and *MC4R* were closely related to obesity (Metherell et al. 2005; Chan et al. 2009), and knock-out of *MC3R* or *MC4R* in mice can also lead to corresponding obesity (Patel et al. 2011). Although both MC3R and MC4R can affect energy homeostasis, their molecular mechanisms were not the same. The main function of MC4R is regulating food intake and energy consumption (Asai et al. 2013). while MC3R mainly regulates energy balance by controlling feed efficiency and circadian rhythm (Girardet and Butler 2014). Additionally, some anti-inflammatory effects of MC3R have been reported recently. (Patel et al. 2011).

The function of MC3R depends on the stimulation of several endogenous ligands (α-, β-, γ-MSH, and ACTH) derived from the pro-opiomelanocortin (POMC), which made the activation of the coupled Gα subunits, in turn, triggers the downstream signal cascade (Cai and Hruby 2016). Studies had found that MC3R can be coupled with Gαs subunits to promote the production of intracellular cyclic adenosine monophosphate (cAMP) and the activation of protein kinase A (PKA) (Yang and Tao 2017). After activation of PKA, it can protect IκB protein from phosphorylation and inhibit the activation of downstream NF-κB signaling pathways (Manna and Aggarwal 1998). In addition, MC3R can also be coupled to Gαi protein to activate MAPK/ERK signaling pathway in 293T cells (Chai et al. 2007).

Although MC3Rs in mammals have been extensively investigated, there are relatively few studies in bony fish. One possible reason is the lack of MC3R in some fishes, such as fugu, medaka (Logan et al. 2003; Klovins et al. 2004a; Selz et al. 2007). As for the tissue expression of *MC3R* in fish, it was currently only reported in spiny dogfish (Klovins et al. 2004b). The pharmacological function, including ligand bind properties and downstream signal regulation, have been studied in a few species of fish, such as red stingray (Takahashi et al. 2016), and channel catfish (Yang et al. 2019). Rainbow trout, a cold-water fish belonging to *Salmonidae*, is one of the most important cultivated fish species in the world with its annual production exceeding 800 thousand tons (FAO 2020). In terms of improving the growth rate and food efficiency of rainbow trout, due to the time-consuming and labor-intensive of traditional selective breeding methods, the endocrine regulation of signal energy metabolism mediated by MC3R is a promising method. In this research, we cloned the coding sequence (CDS) of *rtMC3R* and studied its tissue expression. The cellular function, including the cAMP and MAPK/ERK signaling regulation, were also investigated.

Materials And Methods

2.1 Chemicals, reagents, and primers

The ligands [Nle4, D-Phe7]-α-MSH (NDP-MSH), ACTH (1–24), α-MSH, β-MSH used for pharmacological assays were purchased from GenScript Biotechnology (Nanjing, China). TNF-α was purchased from Sigma Chemical (St. Louis, MO, USA). Primers for conventional PCR and real-time quantitative PCR were designed through primer premier 5 software (PREMIER Biosoft International, Palo Alto, USA) (Table 1), and they were synthesized by Sangon Biotech (Shanghai, China). The restriction enzymes required for molecular cloning were obtained from TaKaRa Biotechnology (Dalian, China).

Table 1
Primers for molecular cloning and quantitative PCR

Primer name	Primer sequence
rtMC3R-F	AAGGCAGTCGTTGTGTGTCT
rtMC3R-R	GCAGCATACGAACACCCCTA
qPCR-F	AAGAACCTCCACTCACCCA
qpcr-R	GACGATGAAGACTATCCCACA
β-actin-F	GGAATCTTGTGGAATCCACGAG
β-actin-R	GGTACATGGTGGTACCTCCAGACAGCA
GADPH-F	AAGCTGGTCACATGGTATGACA
GADPH-R	GGTCACATGACGTAGTTCGGT

2.2 Total RNA extraction

The rainbow trout used in this study were purchased from the Shitou River Rainbow Trout Farm in Shaanxi Province (China), with an average body length of 39 ± 2.5 cm. The fish were anesthetized with ether and then dissected. The tissues, including the kidney, spleen, muscle, stomach, brain, and intestine, were collected to extract total RNA by using the Trizol method.

2.3 Reverse transcription

A total of five μg RNA and 1 μL oligo-deoxythymidine were premixed to a volume of 12 μL. After a short centrifugation, the mix was incubated at 65 ^{0}C for 4 min, and cooled on ice for 2 min. Then 20 mM deoxynucleotide triphosphate (dNTP), 200 U of Moloney murine leukemia virus (M-MLV), and 4μL of 5 x reaction buffer were added into the reaction mix in a total volume of 20 μL. The reverse transcription reaction was performed at 42 ^{0}C for 60 min, followed by a finally heating at 70 ^{0}C for 5min. These reverse-transcribed cDNA samples were used for gene cloning and quantitative real-time PCR of rainbow trout *mc3r*.

2.4 Molecular cloning of rainbow trout *mc3r*

The coding sequence (CDS) of MC3R orthologue (MC3R-like) of rainbow trout was obtained from the National Center for Biological Information (NCBI, https://www.ncbi.nlm.nih.gov/), and then amplified by a PCR reaction. The reaction was conducted in a 10 μL system, which included 20 ng of cDNA template, 0.2 μM of upstream and downstream primers, and 5 μL of 2 x Taq PCR Master Mix (Tiangen, Beijing, China). The amplification parameters are as follows: pre-denaturation at 94 ^{0}C for 5 min; denaturation at 94 ^{0}C for 30 s, annealing at 57 ^{0}C for 30 s, extension at 72 ^{0}C for 1 min, 30 cycles; finally extension at 72 ^{0}C for 10 min before the end of the reaction. Subsequently, 1.5% agarose gel electrophoresis was performed to verify the fragment size, and the PCR product with the expected size was isolated by a DNA gel extraction kit (Tiangen, Beijing, China). The purified DNA fragment was then sub-cloned into the pGEM-T easy vector (Madison, WI, USA) and transformed into *E. coli* (Escherichia coli). Clones containing insert fragments with expected size were sequenced.

2.5 Homology, phylogenetic, and chromosome synteny analysis of rtMC3R

The amino acid sequences of MC3R from different species were multiply aligned according to the sequence similarity by using Clustal Omega (http://www.ebi.ac.uk/Tools/msa/clustalo/). The percentage of similarity was calculated with the same software either. The alignment was colored with DNAMAN 9.0 (LynnonBiosoft, CA, USA). The putative TMDs of rtMC3R were predicted through the online website TMHMM (http://www.cbs.dtu.dk/services/TMHMM/) and NCBI Conserved Domain Search (https://www.ncbi.nlm.nih.gov/Structure/cdd/wrpsb.cgi?). The phylogenetic tree of amino acid was constructed based on the Neighbor-joining (NJ) method (Saitou and Nei, 1987) with Mega X. The strength of the branch relationship was assessed by 1000 bootstrap replications. The chromosome synteny was analyzed with Genomicus (http://www.genomicus.biologie.ens.fr/genomicus) and NCBI genomic browser (https://www.ncbi.nlm.nih.gov).

2.6 Quantitative PCR for tissue distribution of *rtMC3R*

The expression of *rtMC3R* in different tissues was measured by quantitative PCR (qPCR), with the geometric mean of the expression of *β-actin* and *GAPDH* (glyceraldehyde-3-phosphate dehydrogenase) as the internal control (Bustin et al. 2009). The primers used are shown in Table 1. The qPCR was performed on an ECORT48 system in 10 μL reaction volume, containing 50 ng of cDNA template, 0.4 μm of forward and reverse primers, 5 μl of SYBR Green mix, and ddH_2O as volume supplement. The operating parameter was set as follows: 95^0C for 30 s, followed by 30 cycles of 94^0C for 30 s, 54^0C for 30 s, 72^0C for 30 s. The PCR melting curves were depict after amplification. All reactions were carried out in duplicate. The relative expression levels of different tissues were calculated based on the $2^{-\Delta CT}$ method (Schmittgen and Livak 2008). The results were presented as mean ± SEM in arbitrary units (n = 6).

2.7 Cell culture

Human embryonic kidney (HEK) 293T cells, obtained from American Type Culture Collection (ATCC, Manassas, VA, USA), were cultured in Dulbecco's modified Eagle's medium (DMEM, Invitrogen, Carlsbad, CA, USA) containing 10% fetal bovine serum (FBS, Biological Industries, Kibbutz Beit Haemek, Israel) at 37^0C in 5% CO_2-humidified atmosphere. The cells were maintained in a 25 cm^2-cell-culture flask pre-coated with 0.1% gelatin at the density of 2 x 10^5 cells/mL and passaged every 72 h.

2.8 Functional characterization of rtMC3R in HEK293T cells

The functionalities of rtMC3R were examined according to the method established by Ho (2012) with slight modifications. We first sub-cloned the coding sequence of *rtMC3R* into pcDNA3.1 (+), and then co-transfected pcDNA3.1-rtMC3R (prtMC3R) and each of three luciferase reporter vectors into HEK293T cells. The three luciferase reporter gene vectors, pGL4.29, pGL4.33 (Promega, Madison, WI, USA), and pNF-κB-Luc (Clontech, Palo Alto, CA, USA), contain cAMP response element (CRE), serum response element (SRE), and NF-κB (κB) in their promoter regions, respectively, which can monitor the activation of cAMP, MAPK/ERK and NF-KB signaling pathways accordingly. The brief procedure of the test is as follows: the HEK293T cells were passaged to a 6-well plate and grew for 24 hours before transfection. Then the cells were co-transfected using a mixture containing 1000 ng of luciferase reporter vector, 500 ng of receptor expression plasmid (or empty pcDNA3.1), 300 ng of pEGFP-N1 (as an internal control for transfection normalization), and 4 μL of PEI transfection reagent (Fushen Biotechnology, Shanghai, China). The transfected cells were cultured in the original medium for 24 h, and then pipetted down and transplanted in a 48-well plate and incubated at 37°C for another 24 h before ligand treatment. The ligands, such as α-MSH, β-MSH, NDP-MSH, and ACTH (1–24) were diluted by serum-free DMEM medium to the working concentration and then added into the 48-well plate to treat cells for 6 h. After the treatment, cells were lysed with 1 x passive lysis buffer (Beyotime Biotechnology, Shanghai, China), and then luciferase substrate was added for reaction. The luciferase activity was measured with an Infinite F200 microplate reader (Tecan, Männedorf, Switzerland).

2.9 Statistical analysis

The tissue expression of *rtMC3R* uses the $2^{-\Delta CT}$ method to calculate the expression of each tissue relative to the Internal control gene (Schmittgen and Livak, 2008), then uses the one-way ANOVA method to test the equality and Turkey's HSD method was applied for post comparison.

The luciferase activities of the transfected cells treated with different concentrations of ligand were converted into a relative multiple of the treatment group relative to the control group (DMEM serum-free medium). Data analysis was processed by Graphpad Prism 8 software (Graphpad Software, San Diego, CA, USA), and we carried out nonlinear regression analysis, followed by a dose-response-stimulation model. The luciferase activities of the transfected cells treated with TNF-α and MC3R agonist (α-MSH or NDP-MSH) were converted into a change fold of the treatment group relative to the internal control (EGFP). Data were analyzed by the one-way ANOVA method and Turkey's HSD post comparison. For verification results, each test was repeated 3 times.

Results

3.1 Nucleotide and deduced amino acid sequences of rtMC3R

As shown in Fig. 1, the obtained rainbow trout *mc3r* (NCBI accession number: MW884245) contains an open reading frame of 996 bp encoding a putative protein of 331 amino acids. Similar to human MC3R (hMC3R), the receptor we studied had 7 putative hydrophobic transmembrane domains (TMDs). These transmembrane regions were alternately connected by extracellular (ECL) and intracellular (ICL) loops. The two ends of the amino acid were the extracellular N-terminal and the intracellular C-terminal. Three conserved domains PMY, DRY, DPVIY in rtMC3R can be found in TMD2, TMD3, TMD7, respectively. Residues important for ligand binding in hMC3R were also found in rtMC3R, such as E99 (E131 in hMC3R) in TM2, D122 (D154 in hMC3R) and D126 (D158 in hMC3R) in TM3, F261 (F295 in hMC3R) and H264 (H298 in hMC3R) in TM6. Besides, we had discovered 3 N-glycosylation sites (NNT, NET, NIT) in the extracellular N-terminus and 3 phosphorylation sites in the C-terminus through prediction.

Alignment of the amino acid sequence of rtMC3R with other species showed that rtMC3R with that of other fish had high homology (*Oncorhynchus tshawytscha*: 99.7%, *Danio rerio*: 73.85%), whereas the homology of rtMC3R to mammal MC3Rs was relatively low (*Sus scrofa*: 70.67%, *Chelonia mydas*: 70.65%). As shown in Fig. 2, rtMC3R is 31 residues shorter at the N-terminus and 3 residues longer at the C-terminus when compared with human MC3R. The amino acid sequence of rtMC3R was highly consistent in TMDs and ICLs to that of other species while less consistent in N-terminus and ECLs.

3.2 Phylogenetic and chromosome synteny analyses of rtMC3R

We performed phylogenetic analysis on the amino acid sequences of MC3R from different species to assess the evolutionary relationship between the putative rtMC3R and other vertebrate MC3Rs. An NJ tree

based on amino acid sequences of MC3Rs is as shown in Fig. 3. The rtMC3R was nested into the clade of bony fishes and was more evolutionarily related to common salmon *MC3R*.

To determine whether *rtMC3R* was orthologous to the genes in other vertebrates, synteny analysis was performed in Atlantic salmon, channel catfish,zebrafish, humans, horses, and mice. The results were shown in Fig. 4, the adjacent genes of the *rtMC3R*, including *tcf15*, *slc13a3*, and *srxn1*, were consistent with these genes in Atlantic salmon, channel catfish, zebrafish. However, no conserved synteny was observed in adjacent genes of *MC3R* between rainbow trout and mammals

3.3 Tissue expression of rainbow trout *mc3r*

The tissue expression of rainbow trout *mc3r* was analyzed by qPCR. As shown in Fig. 5, the mRNA was predominantly expressed in the brain and muscle, followed by the liver, intestine, gonad, and stomach. The lowest expression was found in the spleen and kidney.

3.4 The functional characteristics of rtMC3R in HEK293T cells

To determine whether rtMC3R can function as a GPCR, rtMC3R was transiently expressed in HEK293T cells and treated with different concentrations of α-MSH, β-MSH, ACTH (1–24), and NDP-MSH. A luciferase reporter vector with a CRE in the promoter (pGL4.29) was used to monitor receptor-mediated cAMP accumulation and pGL4.33 (with SRE in promoter) was used to monitor MAPK/ERK activation. As shown in Figs. 6 and 7, all four agonists can activate cAMP and MAPK/ERK signaling pathways via rtMC3R in a dose-response manner, while the luciferase activity of cells transfected with the empty vector pcDNA3.1 (+) did not appear obvious changes. These four agonists had different potencies for the above two pathways (Table 2). For the cAMP signaling pathway, ACTH (1–24) had the strongest potency (EC_{50} = 6.28 x 10^{-8} μM), followed by NDP-MSH, α-MSH, β-MSH. In terms of the concentration for 50% of maximal effect (EC_{50}) of the MAPK/ERK activation, the order of efficacy was NDP-MSH, β-MSH, α-MSH, ACTH (1–24).

Table2 The signaling properties of rtMC3R in response to ligand stimulation

ligand	cAMP response	ERK1/2 response
	EC_{50}(μm)	EC_{50}(μm)
α-MSH	4.33 ± 1.52	0.50 ± 3.19
β-MSH	9.31 ± 1.57	0.48 ± 2.33
ACTH	0.63 ± 1.01	0.83 ± 3.71
NDP-MSH	2.93 ± 6.47	0.09 ± 1.09

Values were expressed as the mean ± SEM of at least three independent experiments. Abbreviations: α-MSH (α-melanocyte-stimulating hormone), β-MSH (β-melanocyte-stimulating hormone), ACTH (Adrenocorticotropic Hormone), NDP-MSH ([Nle4, D-Phe7]-MSH). EC50were calculated from fitting curves based on triplicate measurements within 1 experiment.

To determine whether *rtMC3R* was involved in regulating the NK-κB signaling pathway, we co-transfected HEK293T cells with prtMC3R and the luciferase reporter genes pNFκB-Luc which had NF-κB enhancer elements upstream of the promoter. Results showed that (Fig. 8), cells transfected with prtMC3R could significantly inhibit TNF-α induced NF-κB elevation, whereas cells transfected with pcDNA3.1 (+) empty vector have no similar results. In addition, NDP-MSH showed a better inhibitory effect than α-MSH.

Discussion

Studies in mammals have confirmed that MC3R and MC4R are regulators of energy homeostasis. Unlike MC4R, which is regulated by leptin and influences food intake and energy expenditure (Asai et al. 2013), MC3R mainly participates in the regulation of energy homeostasis by affecting food intake efficiency (Girardet and Butler 2014). Besides, MC3R is involved in the regulation of immunity (Patel et al. 2011). For instance, in both allergic and non-allergic mice models of lung inflammation, melanocortin peptides can inhibit leukocyte accumulation by activating MC3R (Getting et al. 2008). Till now, extensive studies on MC3R have been carried out in mammals, including panda (Zhang et al. 2019), mice (Lee et al. 2016), pig (Fan et al. 2008), etc. However, this receptor has only been studied in a few species of fish, such as channel fish (Yang et al. 2019) and some cartilaginous fishes (Klovins et al. 2004b; Takahashi et al. 2016). Rainbow trout, as a world-renowned cold-water economic fish, has received considerable attention for its energy and immune regulation. In this study, we cloned the CDS of rtMC3R, investigated its tissue expression profile, and characterized the activation of its downstream signals.

The obtained cDNA was *rtMC3R* based on several structural features and multiple sequence alignments (Fig. 1 and Fig. 2). The amino acid sequence of rtMC3R was highly conserved at 7 transmembrane domains (7 TMDs), which were essential for ligand binding and activation of downstream signals (Yang et al. 2000). In addition, rtMC3R has 3 conserved motifs similar to mammalian MC3Rs, which are PMY, DRY, and DPxxY (Huang and Tao 2014; Yang et al. 2015). It worth noting that the NPxxY motif only in rainbow trout and Chinook salmon is DPVIY, while in humans (*Homo sapiens*), mouse (*Mus musculus*), western clawed frog (*Xenopus tropicalis*), and zebrafish (*Danio rerio*) is DPLIY, showing a unique evolutionary status of salmonids. Multiple sequence alignment of MC3R in different species showed that the sequence identity between rtMC3R and several bony fish exceeded 90%. The sequence identity with hMC3R is also as high as 73.5%, indicating that MC3R is highly conserved among species. In addition to the highly conserved regions in TMDs and ECLs, lower sequence homology in the N-terminus, C-terminus, and ICL3 was also observed, implying that rtMC3R may have unique pharmacology as MC4Rs studied in other fish (Li et al. 2016, 2017).

We also predicted N-glycosylation and phosphorylation sites through online tools. The N-glycosylation of protein generally recognizes a specific Asn-X-Ser/Thr (NXS/T) motif. In GPCRs, this modification is involved in normal protein folding, cell surface expression, ligand binding, and downstream signal transduction (Chen et al. 2010). Through NetNGlyc 1.0 server, we found 3 N-glycosylation sites located before TMD1 in rtMC3R, which is consistent with hMC3R. The difference is that the sequences of the three potential glycosylation sites in rtMC3R are NNT, NET, and NLT, while the motifs recognized in hMC3R are NAS, NGS, and NQS. The phosphorylation of GPCRs mainly occurs at the C-terminus and ICLs, which will cause the GPCR to uncouple from its cognate G protein and GPCR desensitization (Lefkowitz 1998). The phosphorylated sites will then recruit arrestins, and the number of phosphorylated sites and phosphorylation barcodes will induce different conformational states of arrestins, leading to different cell outcomes (Wilden 1995; Mendez et al. 2000; Vishnivetskiy et al. 2007; Butcher et al. 2011; Liggett 2011; Prihandoko et al. 2015). In this study, we found 3 potential phosphorylation sites at the C-terminus of rtMC3R, and their arrangement is similar to hMC3R, suggesting that rtMC3R may have similar desensitization and G protein-independent signal regulation mechanisms with hMC3R (Fig. 1). Moreover, several residues that were important for ligand recognition in hMC3R were also found in rtMC3R, including E99, D122, D126, F261, and H264, which implies rtMC3R might have similar ligand-binding sites to hMC3R (Yang and Harmon 2017).

Phylogenetic analysis based on amino acid sequence showed that the MC3Rs of mammals, amphibians, and bony fishes were clustered into three groups respectively, which were consistent with their evolutionary status, and rtMC3R was classified into teleost MC3R subtype. Synteny analysis further demonstrated that genes surrounding *mc3r* in rainbow trout are highly conserved compared with Atlantic salmon, channel catfish, and zebrafish, but different from those in mammals. These data together revealed the evolutionary conservation of MC3Rs in fish.

In mammals, MC3R is mainly expressed in the central nervous system (CNS), peripheral tissues, and immune cells, including the brain, intestine, placenta, etc. (Gantz et al. 1993), and is involved in the regulation of energy metabolism, cardiovascular function, and inflammation (Getting 2006). In this study, we used real-time qPCR to detect the tissue expression of rainbow trout *mc3r* mRNA. Results (Fig. 5) showed that rainbow trout *mc3r* was predominantly expressed in the brain, consistent with the studies in mammals (Gantz and Fong 2003) and some cartilaginous fishes, such as spiny dogfish (*Squalus acanthias*) (Klovins et al. 2004b) and stingray (*Dasyatis akajei*) (Takahashi et al. 2016), suggesting rtMC3R may be involved in the CNS-regulated energy homeostasis. The mRNA was also highly expressed in muscle, similar to the results obtained in *Megalobrama amblycephala* (Liao et al. 2019). Moreover, the mRNA of this gene can also be detected in the stomach, liver, gonad, intestine, and kidney. Of them, the liver, kidney, and intestine are crucial immune organs in fish, showing that rtMC3R may also participate in the regulation of inflammatory response as in mammals.

Mammalian MC3R is coupled to Gαs protein and can activate cAMP and MAPK/ERK signaling pathways (Lee et al. 2001; Chai et al. 2007). To determine whether rtMC3R has similar functions, we used the luciferase reporter system to detect the activity of the cAMP and MAPK signaling pathways after

treatment with four different agonists. Results showed that ACTH (1–24) had the highest potency in activating the cAMP signaling pathway, followed by NDP-MSH, α-MSH, and β-MSH. The high activation efficacy of ACTH (1–24) in this study is similar to that of channel catfish (Yang et al. 2019) but is different from that of pigs (Fan et al. 2008). As a “primitive” ligand, ACTH (1–24) exhibits a high affinity for MCRs of fishes (Klovins et al., 2004b; Li et al., 2016), but a relatively low affinity for MCRs of mammals (Lisak and Benjamins 2017). Our results provide another evidence to support the concept that ACTH may be the “original” ligand for the ancestral melanocortin receptors (Dores and Baron 2011; Dores et al. 2014). MAPK/ERK signals are involved in the regulation of energy homeostasis (Yang and Tao 2017). In this study, we found that the synthetic ligand NDP-MSH has a higher activation potency for the MAPK/ERK signal pathway than the endogenous ligands, which is similar to that of mammals (Fan et al. 2008). The different activation efficacies of the four ligands on cAMP and MAPK/ERK signals suggest that the structural differences between fish and mammalian MC3R may bring about different receptor conformation and downstream signal transduction.

The NF-κB signaling system is composed of NF-κB dimer, I-κB modulator, and IKK. If the NF-κB signaling system received specific signals and was activated, some physiological or immune processes wound occur, such as inflammation, immunity, oxidative stress, etc. (Mitchell et al. 2016). Researchers had reported that human MC3R, once activated by ligands, can activate PKA by elevating cAMP level, and protected IκB protein from phosphorylation, thereby inhibiting NF-κB nuclear translocation (Manna and Aggarwal 1998). In this study, we added a premix of NDP-MSH or α-MSH and TNF-α to the cells transfected with rtMC3R and found that activated rtMC3R inhibited the signal of NF-κB (Fig. 8). The results were similar to those observed in human central and peripheral nervous systems of human (Ichiyama et al. 1999; Teare et al. 2004), confirmed that rtMC3R also has an anti-inflammatory function after activation.

In conclusion, we cloned the evolutionarily highly conserved rainbow trout *mc3r* and investigated its tissue expression and signaling properties. This gene was highly expressed in the brain and muscle and was also widely expressed in other peripheral tissues. Functional studies on cells indicated that endogenous and synthetic ligands can activate cAMP and MAPK/ERK signaling pathways through rtMC3R with different potencies. Inflammation-related NF-κB signal pathway was also mediated by rtMC3R. Future studies will be carried out to elucidate the function of rtMC3R in the muscle and peripheral tissues of rainbow trout.

Declarations

Acknowledgments

We are grateful for the methodological guidance by Prof. Ya-Xiong Tao at Auburn University.

Authors’ contributions

Li-Xin Wang conceived and designed this study; Hui-Xia Yu and Yang Li cloned rainbow trout *mc3r*, performed the cellular experiment, and prepared the manuscript; Wei-Jia Song, Hui Wang, and Hao-Lin Mo collected the samples; Qiao Liu, Xin-Miao Zhang, Ze-Bin Jiang extracted RNA and examined the tissue distribution of rtMC3R.

Funding

This research was supported by the National Natural Science Foundation of China (No. 31502180), Shaanxi Provincial Water Conservancy Science and Technology Fund (No. 2016slkj-16), Shaanxi Provincial Agricultural Products Quality and Safety Project, partially supported by the National Key R&D Program of China (2019YFD0900200).

Data availability

The data and materials that support the findings of this study are available from the corresponding author upon reasonable request.

Compliance with ethical standards

Conflict of interest

The authors declare that they have no conflict of interest.

Ethics declarations

The Faculty Animal Policy and Welfare Committee of Northwest A&F University under contract (NWAFU-314020038) approved this experiment, and the experimental process complied with protocols of international guidelines for the ethical use of animals in research.

References

1. Asai M, Ramachandrappa S, Joachim M et al (2013) Loss of function of the melanocortin 2 receptor accessory protein 2 is associated with mammalian obesity. Science 341:275–278. https://doi.org/10.1126/science.1233000
2. Bustin SA, Benes V, Garson JA et al (2009) The MIQE guidelines: minimum information for publication of quantitative real-time PCR experiments. Clin Chem 55:611–622. https://doi.org/10.1373/clinchem.2008.112797
3. Butcher AJ, Prihandoko R, Kong KC et al (2011) Differential G-protein-coupled receptor phosphorylation provides evidence for a signaling bar code. J Biol Chem 286:11506–11518. https://doi.org/10.1074/jbc.M110.154526
4. Cai M, Hruby VJ (2016) The Melanocortin Receptor System: A Target for Multiple Degenerative Diseases. Curr Protein Pept Sci 17:488–496. https://doi.org/10.2174/1389203717666160226145330

5. Chai B, Li J-Y, Zhang W et al (2007) Melanocortin-3 receptor activates MAP kinase via PI3 kinase. Regul Pept 139:115–121. https://doi.org/https://doi.org/10.1016/j.regpep.2006.11.003
6. Chan LF, Webb TR, Chung TT et al (2009) MRAP and MRAP2 are bidirectional regulators of the melanocortin receptor family. Proc Natl Acad Sci U S A 106:6146–6151. https://doi.org/10.1073/pnas.0809918106
7. Chen Q, Miller LJ, Dong M (2010) Role of N-linked glycosylation in biosynthesis, trafficking, and function of the human glucagon-like peptide 1 receptor. Am J Physiol - Endocrinol Metab 299:62–68. https://doi.org/10.1152/ajpendo.00067.2010
8. Dores RM, Baron AJ (2011) Evolution of POMC: origin, phylogeny, posttranslational processing, and the melanocortins. Ann N Y Acad Sci 1220:34–48. https://doi.org/10.1111/j.1749-6632.2010.05928.x
9. Dores RM, Londraville RL, Prokop J et al (2014) Molecular evolution of GPCRs: Melanocortin/melanocortin receptors. J Mol Endocrinol 52:T29–T42. https://doi.org/10.1530/JME-14-0050
10. Fan ZC, Sartin JL, Tao YX (2008) Molecular cloning and pharmacological characterization of porcine melanocortin-3 receptor. J Endocrinol 196:139–148. https://doi.org/10.1677/JOE-07-0403
11. FAO (2020) The State of World Fisheries and Aquaculture 2020. Sustainability in action
12. Gantz I, Fong TM (2003) The melanocortin system. Am J Physiol Metab 284:E468–E474. https://doi.org/10.1152/ajpendo.00434.2002
13. Gantz I, Konda Y, Tashiro T et al (1993) Molecular cloning of a novel melanocortin receptor. J Biol Chem 268:8246–8250. https://doi.org/10.1016/s0021-9258(18)53088-x
14. Getting SJ (2006) Targeting melanocortin receptors as potential novel therapeutics. Pharmacol Ther 111:1–15. https://doi.org/10.1016/j.pharmthera.2005.06.022
15. Getting SJ, Riffo-Vasquez Y, Pitchford S et al (2008) A role for MC3R in modulating lung inflammation. Pulm Pharmacol Ther 21:866–873. https://doi.org/https://doi.org/10.1016/j.pupt.2008.09.004
16. Girardet C, Butler AA (2014) Neural melanocortin receptors in obesity and related metabolic disorders. Biochim Biophys Acta - Mol Basis Dis 1842:482–494. https://doi.org/https://doi.org/10.1016/j.bbadis.2013.05.004
17. Ho JCW, Jacobs T, Wang Y, Leung FC (2012) Identification and characterization of the chicken galanin receptor GalR2 and a novel GalR2-like receptor (GalR2-L). Gen Comp Endocrinol 179:305–312. https://doi.org/10.1016/j.ygcen.2012.09.005
18. Huang H, Tao Y-X (2014) Functions of the DRY motif and intracellular loop 2 of human melanocortin 3 receptor. J Mol Endocrinol 53:319–330. https://doi.org/10.1530/JME-14-0184
19. Ichiyama T, Campbell IL, Furukawa S, et al (1999) Autocrine α-melanocyte-stimulating hormone inhibits NF-κB activation in human glioma. J Neurosci Res 58:684–689. https://doi.org/10.1002/(SICI)1097-4547(19991201)58:5<684::AID-JNR9>3.0.CO;2-%23

20. Klovins J, Haitina T, Fridmanis D et al (2004a) The Melanocortin System in Fugu: Determination of POMC/AGRP/MCR Gene Repertoire and Synteny, As Well As Pharmacology and Anatomical Distribution of the MCRs. Mol Biol Evol 21:563–579. https://doi.org/10.1093/molbev/msh050
21. Klovins J, Haitina T, Ringholm A et al (2004b) Cloning of two melanocortin (MC) receptors in spiny dogfish: MC3 receptor in cartilaginous fish shows high affinity to ACTH-derived peptides while it has lower preference to γ-MSH. Eur J Biochem 271:4320–4331. https://doi.org/10.1111/j.1432-1033.2004.04374.x
22. Lee B, Koo J, Yun Jun J et al (2016) A mouse model for a partially inactive obesity-associated human MC3R variant. Nat Commun 7:10522. https://doi.org/10.1038/ncomms10522
23. Lee EJ, Lee S, Jung J et al (2001) Differential regulation of cAMP-mediated gene transcription and ligand selectivity by MC3R and MC4R melanocortin receptors. Eur J Biochem 268:582–591. https://doi.org/10.1046/j.1432-1327.2001.01900.x
24. Lefkowitz RJ (1998) G protein-coupled receptors: III. New roles for receptor kinases and β- arrestins in receptor signaling and desensitization. J Biol Chem 273:18677–18680. https://doi.org/10.1074/jbc.273.30.18677
25. Li JT, Yang Z, Chen HP et al (2016) Molecular cloning, tissue distribution, and pharmacological characterization of melanocortin-4 receptor in spotted scat, Scatophagus argus. Gen Comp Endocrinol 230–231:143–152. https://doi.org/10.1016/j.ygcen.2016.04.010
26. Li L, Yang Z, Zhang YP et al (2017) Molecular cloning, tissue distribution, and pharmacological characterization of melanocortin-4 receptor in grass carp (Ctenopharyngodon idella). Domest Anim Endocrinol 59:140–151. https://doi.org/10.1016/j.domaniend.2016.11.004
27. Liao S, Chen K, Xi B et al (2019) Molecular cloning, characterization, and expression analysis of Megalobrama amblycephala melanocortin receptor 3 during fasting. J Fish Sci China 26:445–456. https://doi.org/10.3724/SP.J.1118.2019.18262
28. Liggett SB (2011) Phosphorylation barcoding as a mechanism of directing GPCR signaling. Sci Signal 4:2–5. https://doi.org/10.1126/scisignal.2002331
29. Lisak RP, Benjamins JA (2017) Melanocortins, melanocortin receptors and multiple sclerosis. Brain Sci 7:1–18. https://doi.org/10.3390/brainsci7080104
30. Logan DW, Bryson-Richardson RJ, Pagán KE et al (2003) The structure and evolution of the melanocortin and MCH receptors in fish and mammals. Genomics 81:184–191. https://doi.org/https://doi.org/10.1016/S0888-7543(02)00037-X
31. Manna SK, Aggarwal BB (1998) α-Melanocyte-stimulating hormone inhibits the nuclear transcription factor NF-κB activation induced by various inflammatory agents. J Immunol 161:2873–2880. https://doi.org/10.1097/00005768-199905001-00697
32. Mendez A, Burns ME, Roca A et al (2000) Rapid and reproducible deactivation of rhodopsin requires multiple phosphorylation sites. Neuron 28:153–164. https://doi.org/10.1016/S0896-6273(00)00093-3

33. Metherell LA, Chapple JP, Cooray S et al (2005) Mutations in MRAP, encoding a new interacting partner of the ACTH receptor, cause familial glucocorticoid deficiency type 2. Nat Genet 37:166–170. https://doi.org/10.1038/ng1501
34. Mitchell S, Vargas J, Hoffmann A (2016) Signaling via the NFκB system. WIREs Syst Biol Med 8:227–241. https://doi.org/https://doi.org/10.1002/wsbm.1331
35. Novoselova TV, Chan LF, Clark AJL (2018) Pathophysiology of melanocortin receptors and their accessory proteins. Best Pract Res Clin Endocrinol Metab 32:93–106. https://doi.org/https://doi.org/10.1016/j.beem.2018.02.002
36. Patel H, Montero-Melendez T, Greco K, Perretti M (2011) Melanocortin Receptors as Novel Effectors of Macrophage Responses in Inflammation. Front Immunol 2:41. https://doi.org/10.3389/fimmu.2011.00041
37. Prihandoko R, Bradley SJ, Tobin AB, Butcher AJ (2015) Determination of GPCR phosphorylation status: Establishing a phosphorylation barcode. Curr Protoc Pharmacol 2015:2.13.1–2.13.26. https://doi.org/10.1002/0471141755.ph0213s69
38. Schmittgen TD, Livak KJ (2008) Analyzing real-time PCR data by the comparative CT method. Nat Protoc 3:1101–1108. https://doi.org/10.1038/nprot.2008.73
39. Selz Y, Braasch I, Hoffmann C et al (2007) Evolution of melanocortin receptors in teleost fish: The melanocortin type 1 receptor. Gene 401:114–122. https://doi.org/https://doi.org/10.1016/j.gene.2007.07.005
40. Takahashi A, Davis P, Reinick C et al (2016) Characterization of melanocortin receptors from stingray Dasyatis akajei, a cartilaginous fish. Gen Comp Endocrinol 232:115–124. https://doi.org/https://doi.org/10.1016/j.ygcen.2016.03.030
41. Teare KA, Pearson RG, Shakesheff KM, Haycock JW (2004) Alpha-MSH inhibits inflammatory signalling in Schwann cells. Neuroreport 15:493–498. https://doi.org/10.1097/00001756-200403010-00022
42. Vishnivetskiy SA, Raman D, Wei J et al (2007) Regulation of arrestin binding by rhodopsin phosphorylation level. J Biol Chem 282:32075–32083. https://doi.org/10.1074/jbc.M706057200
43. Wilden U (1995) Duration and Amplitude of the Light-Induced cGMP Hydrolysis in Vertebrate Photoreceptors Are Regulated by Multiple Phosphorylation of Rhodopsin and by Arrestin Binding. Biochemistry 34:1446–1454. https://doi.org/10.1021/bi00004a040
44. Yang L, Tao Y (2017) Biased signaling at neural melanocortin receptors in regulation of energy homeostasis. Biochim Biophys Acta - Mol Basis Dis 1863:2486–2495. https://doi.org/10.1016/j.bbadis.2017.04.010
45. Yang L, Zhang Z, Wen H, Tao Y (2019) Characterization of channel catfish (Ictalurus punctatus) melanocortin-3 receptor reveals a potential network in regulation of energy homeostasis. Gen Comp Endocrinol 277:90–103. https://doi.org/10.1016/j.ygcen.2019.03.011
46. Yang Y, Fong TM, Dickinson CJ et al (2000) Molecular determinants of ligand binding to the human melanocortin-4 receptor. Biochemistry 39:14900–14911. https://doi.org/10.1021/bi001684q

47. Yang Y, Harmon CM (2017) Molecular signatures of human melanocortin receptors for ligand binding and signaling. Biochim Biophys Acta (BBA)-Molecular Basis Dis 1863:2436–2447. https://doi.org/10.1016/j.bbadis.2017.04.025
48. Yang Z, Huang Z, Tao Y (2015) Functions of DPLIY motif and helix 8 of human melanocortin-3 receptor. J Mol Endocrinol 55:107. https://doi.org/10.1530/JME-15-0116
49. Zhang H, Xie H, Wang W et al (2019) Pharmacology of the giant panda (Ailuropoda melanoleuca) melanocortin-3 receptor. Gen Comp Endocrinol 277:73–81. https://doi.org/https://doi.org/10.1016/j.ygcen.2018.10.024

Figures

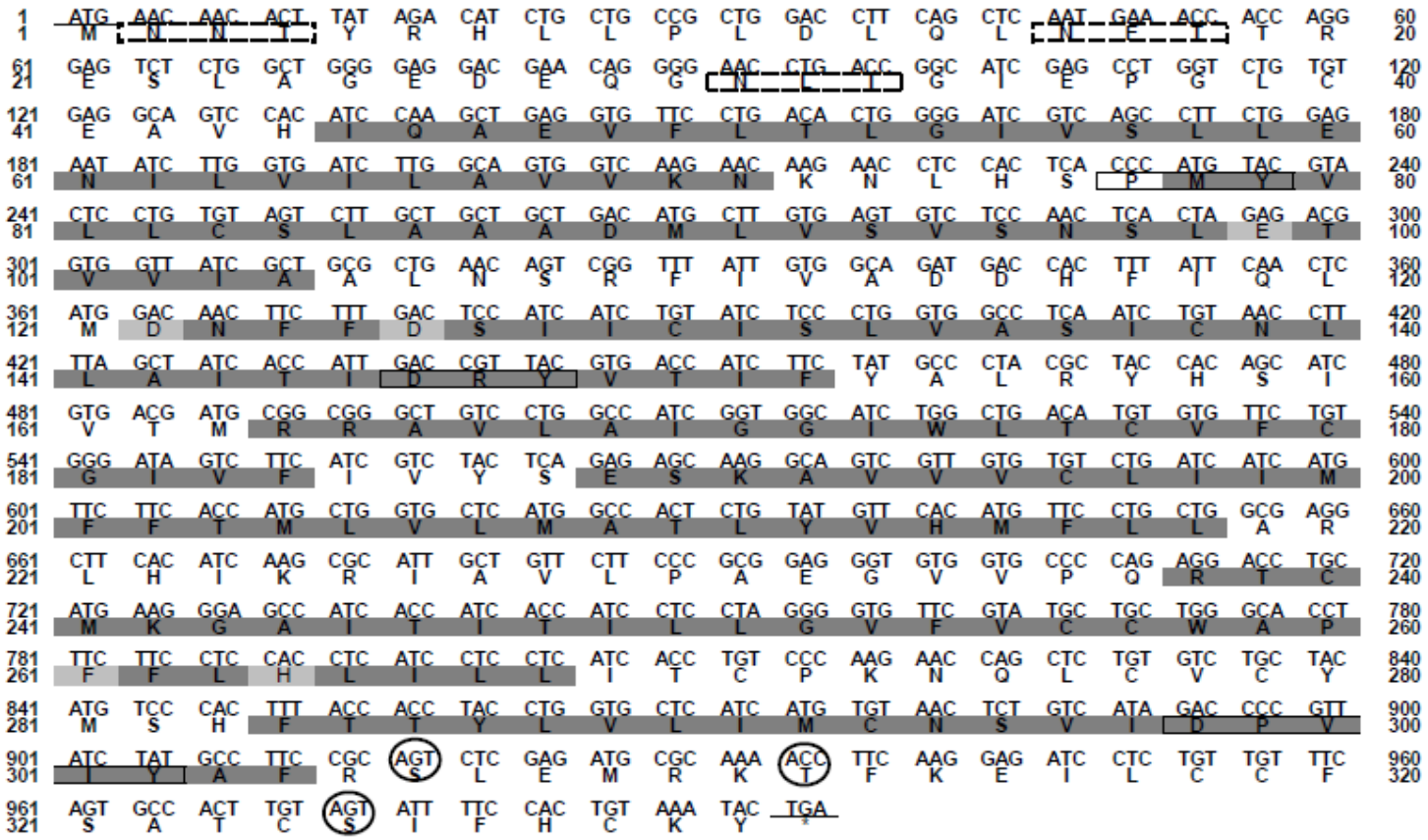

Figure 1

Nucleotide sequence of rtMC3R and its deduced amino acid sequence. The position information of nucleotides and amino acids was marked on both sides. Dark gray shading indicates 7 transmembrane structure regions, and three conserved motifs were highlighted with black solid boxes (PMY, DRY, DPVIY). The glycosylation site at the N-terminus was shown in the dashed box. Amino acid residues important for ligand binding were filled with light gray. The phosphorylation site at the C-terminus was highlighted with black circles. The initiation codon (ATG) and a termination codon (TAG) were underlined.

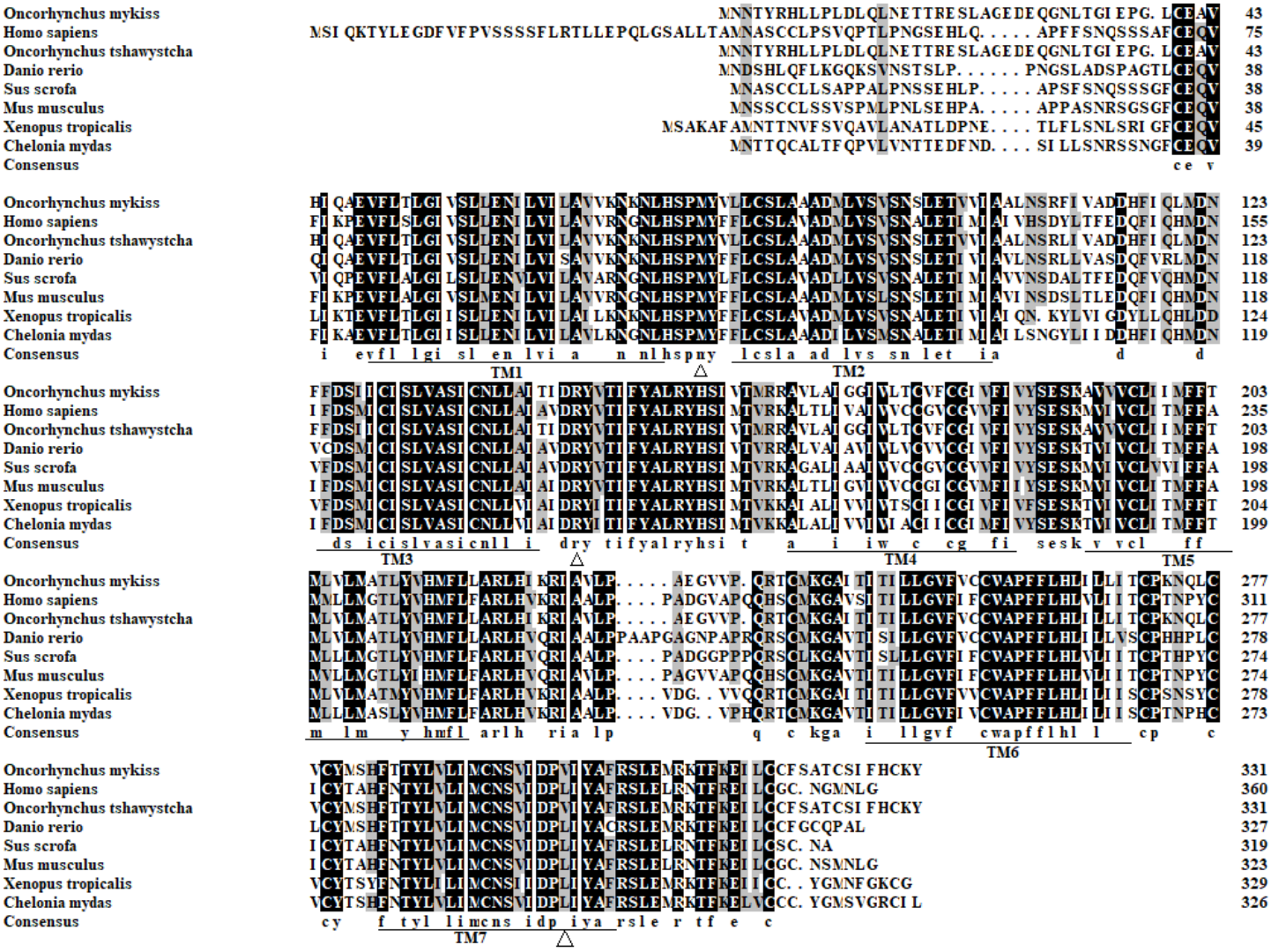

Figure 2

Multiple sequence alignments of the deduced amino acid sequence of rainbow trout MC3R with other species. Single underlining indicated the seven predicted TMDs, The triangle symbol was adopted to mark the three conserved motifs (PMD, DRY, DPVIY)

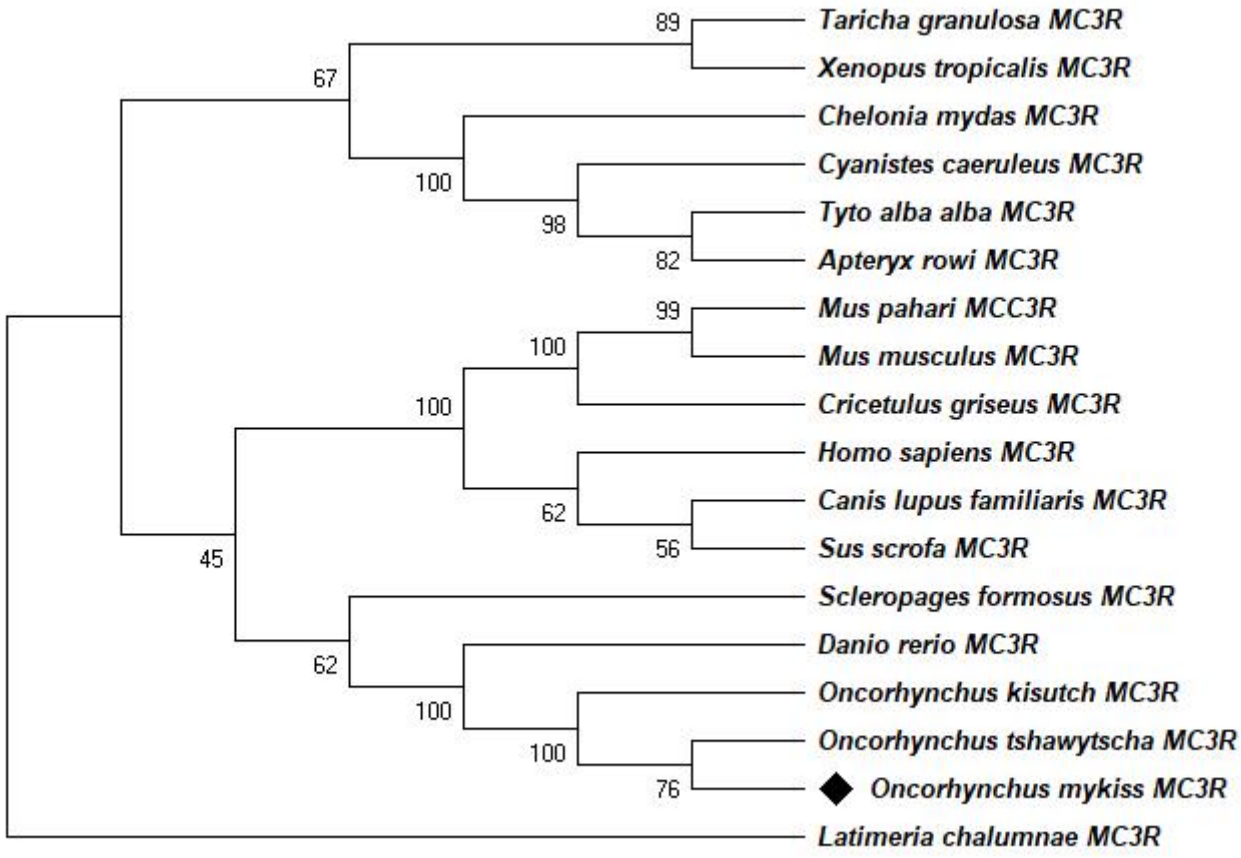

Figure 3

Phylogenetic tree of MC3Rs. The tree was constructed using the Neighbor-Joining (NJ) method. The number on the node represents the guide value (expressed as a percentage) obtained for 1000 repetitions. The diamond indicates rtMC3R. MCRs: Oncorhynchus tshawytscha (XP_024229914.1), Oncorhynchus kisutch (XP_020360426.1), Scleropages formosus (XP_018615783.1), Chelonia mydas (XP_007059824.1), Mus pahari (XP_021049931.1), Taricha granulosa (AAX18229.1), Canis lupus familiaris (NP_001128596.1), Cricetulus griseus (XP_003501490.1), Tyto alba alba (XP_009967958.1), Apteryx rowi (XP_025911964.1), Cyanistes caeruleus (XP_023795719.1), Latimeria chalumane (XP_005990660.1), Chelonia mydas (XP_007059824.1), Homo sapiens (AKI72214.1), Mus musculus (NP_032587.1), Sus scrofa (AFK25142.1), Danio rerio (AAI62747.1), Xenopus tropicalis (XP_002935436.1).

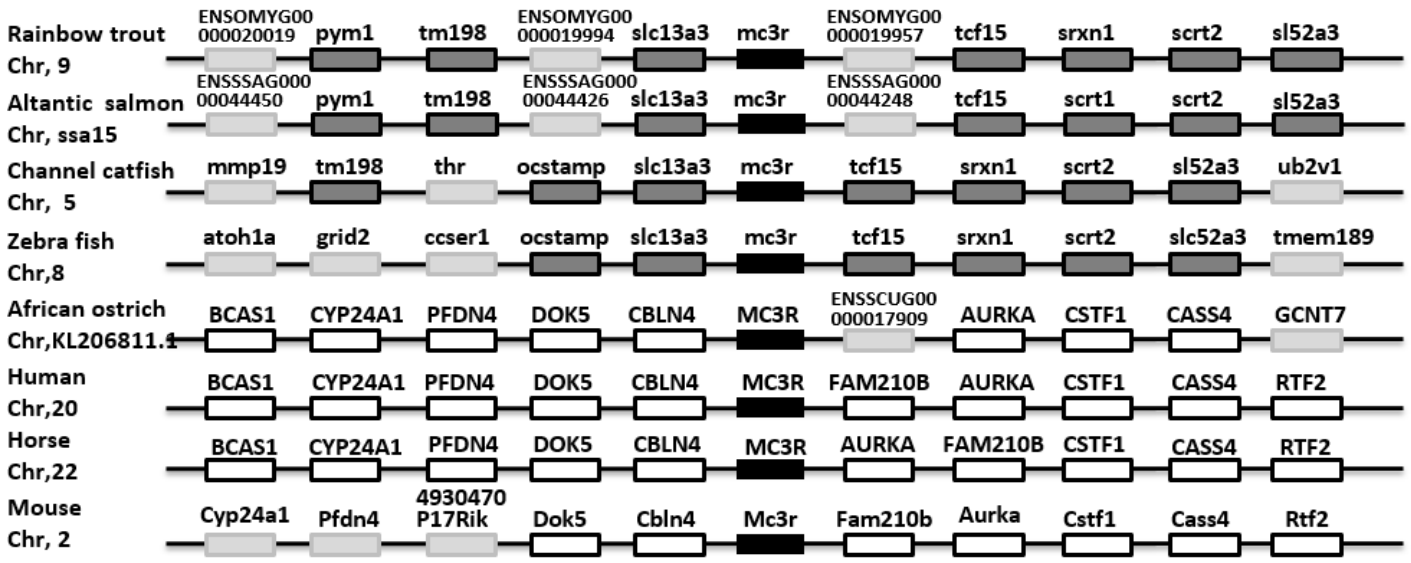

Figure 4

Chromosome synteny analysis of MC3Rs in different species. The syntenic genes were represented by boxes and connected by black lines. The MC3R genes were indicated by black-filled box. The conserved synteny of fish were represented by dark gray boxes, while in other species they were filled with white. Unknown genes were highlighted in light gray boxes.

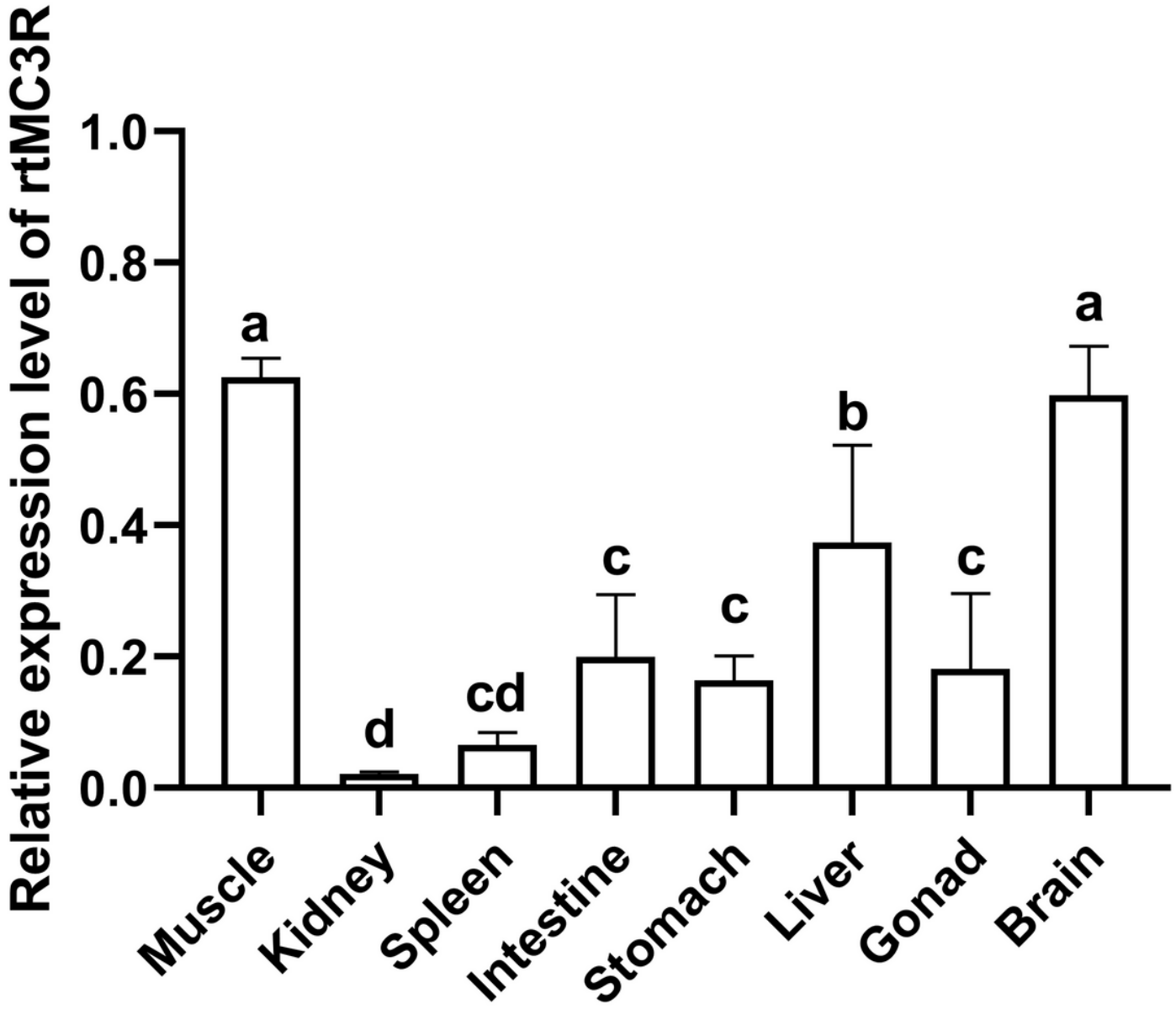

Figure 5

Relative expression of rtMC3R in various tissues. Two reference genes, β-actin and GAPDH were used as the internal controls. The results were presented by the relative expression of each tissue to the internal controls. The same lowercase letters indicated no significant difference, while different lowercase letters indicated significant difference, and the test level was 0.05.

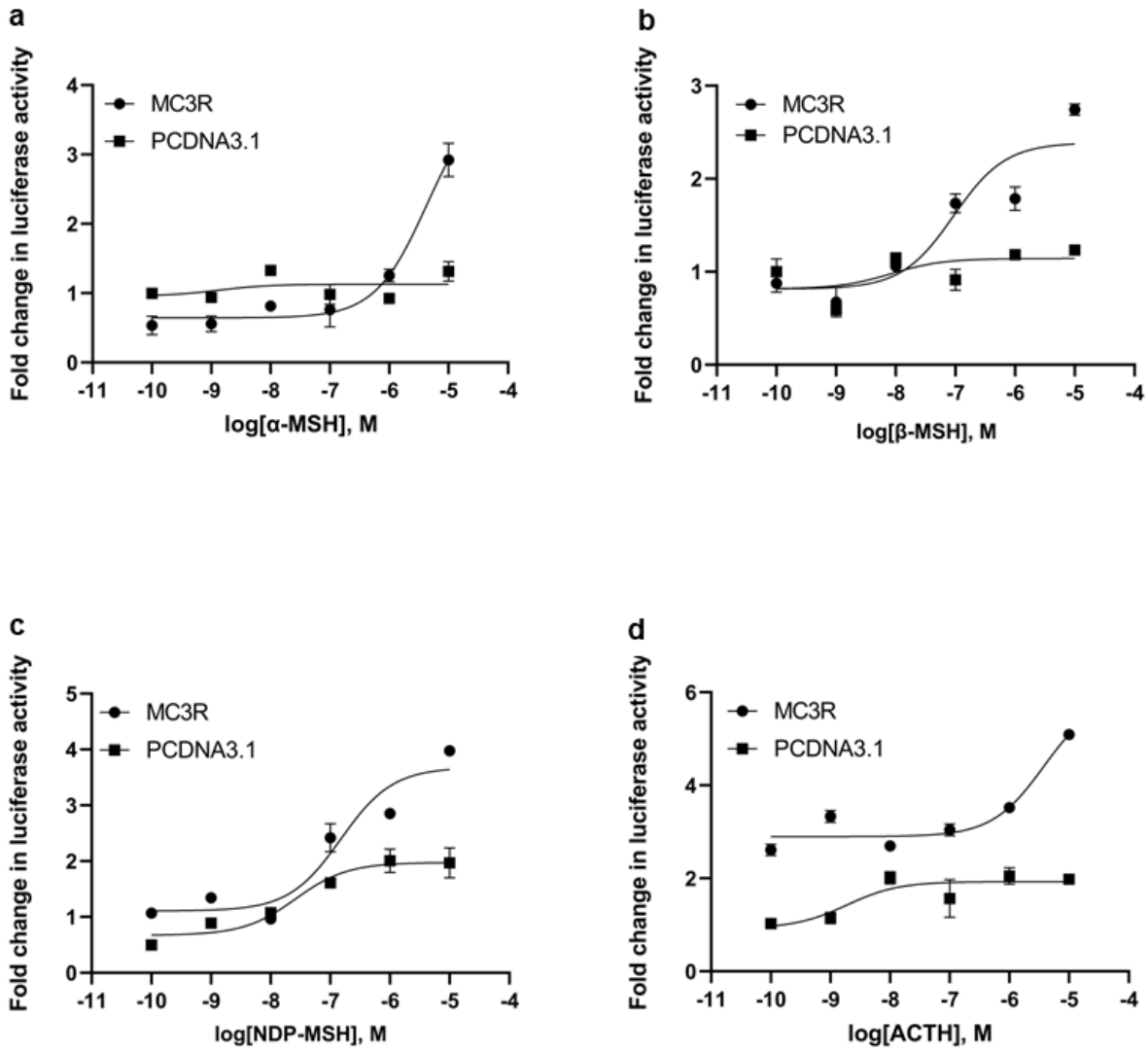

Figure 6

The cAMP signaling of rtMC3R in HEK293 cells. After stimulating cells with different concentrations of (a) α-MSH, (b) β-MSH, (c) NDP-MSH and (d) ACTH (1-24), the luciferase activity of the cAMP signaling pathway was detected. The results were presented as fold change of the treatment group relative to the control group (DMEM serum-free medium). Each data point represents the mean ± SEM of three repeated measurements.

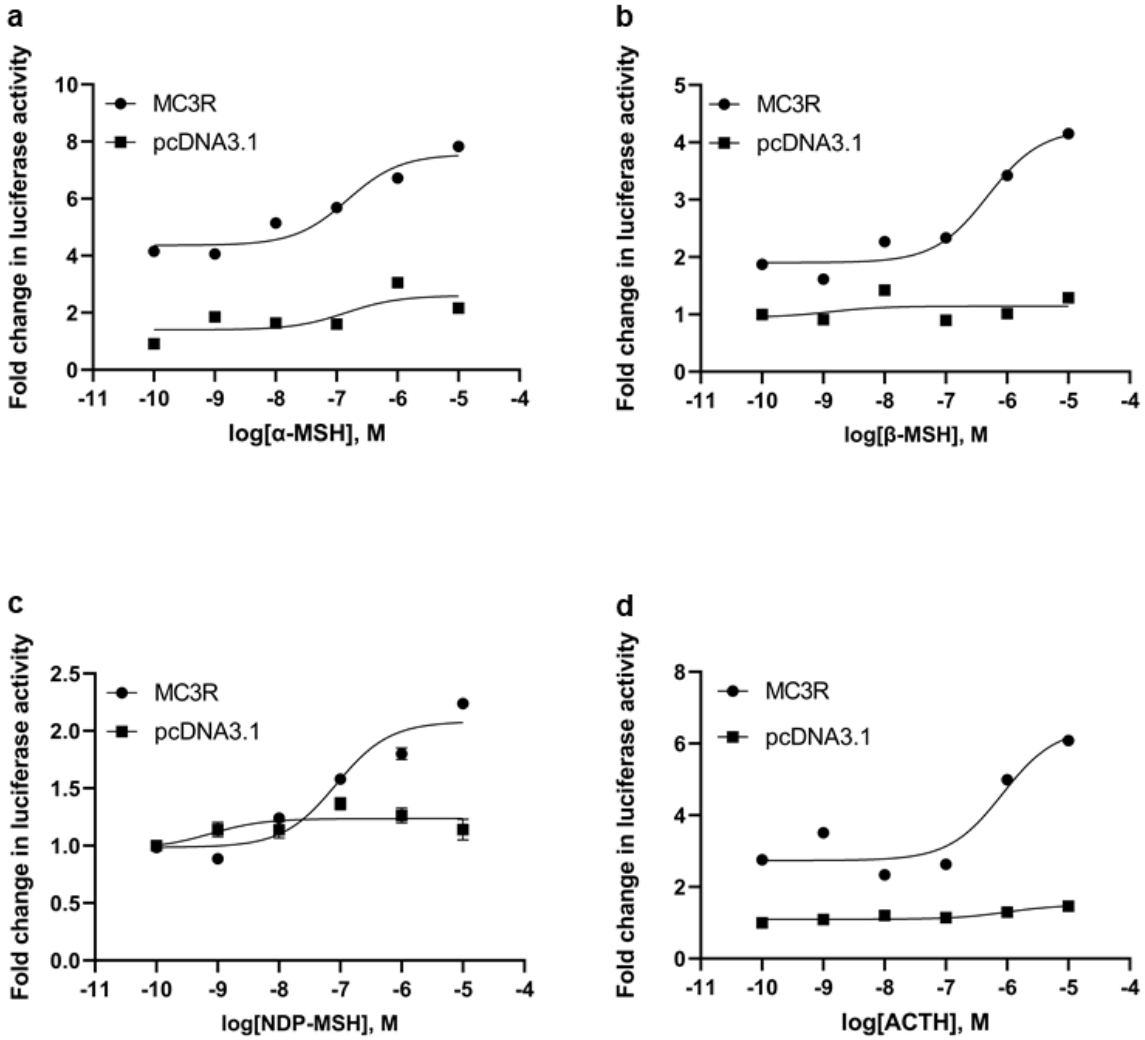

Figure 7

MAPK/ERK signaling of rtMC3R in HEK293 cells. Forty eight hours after plasmids (prtMC3R and pGL4.33) transfection, the HEK293 were treated with different concentrations of (a) α-MSH, (b) β-MSH, (c) NDP-MSH and (d) ACTH (1-24), and the activation of ERK1/2 signaling was detected by a single luciferase reporter system. Data points represented the mean ± SEM of three repeated measurements.

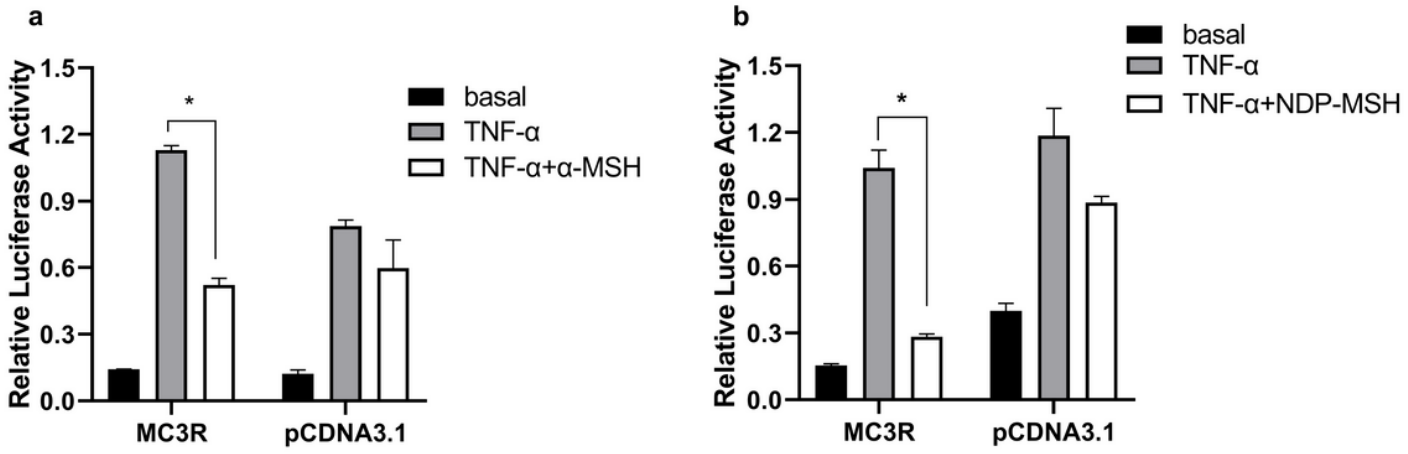

Figure 8

NF-κB signaling of rtMC3R in HEK293 cells. HEK293 cells were co-transfected with prtMC3R and pNF-KB, and then TNF-α as well as two different agonists (α-MSH and NDP-MSH) were added into the medium for 6 h. After the treatment, cells were lyzed and luciferase activities were analyzed. Data points represented the mean ± SEM of three repeated measurements and statistics were performed by one-way ANOVA. * $P < 0.05$